Front. Chem. China 2008, 3(4): 458–463
DOI 10.1007/s11458-008-0081-5

RESEARCH ARTICLE

Yin PENG, Ling BAO

Controlled-synthesis of ZnO nanorings

Abstract ZnO nanorings were synthesized on a large scale by an easy solution-based method at 70°C for 5 h using hexamethylenetramine ($C_6H_{12}N_4$, HMT) and Zn $(NO_3)_2 \cdot 2H_2O$ as raw materials in the presence of surfactant poly(acrylamide-*co*-diallyldimethylammonium chloride) (PAM-CTAC). The structure and morphology of the products were characterized by X-ray powder diffraction (XRD) and scanning electron microscopy (SEM). The influence of experimental conditions such as concentration of surfactant and reactants, reaction temperature on the structure and morphology of the products were investigated. A probable formation mechanism of ZnO nanorings in the presence of surfactant PAM-CTAC was discussed. The results show that the products are wurtzite hexagonal ZnO nanorings with an inner diameter of 220 nm and a wall thickness of 70 nm. Reaction temperature and concentration of reactants influence the shape and size of ZnO nanorings but PAM-CTAC plays the key role in the formation of ZnO nanorings. Through adjusting the concentration of PAM-CTAC, controlled-synthesis of ZnO nanorings can be realized. A room temperature photoluminescence (PL) spectrum of ZnO obtained shows that the full width at half maximum (FWHM) of the UV emission (~ 7 nm) is much narrower than that of commercial ZnO bulk crystals (~ 18 nm). The narrow FWHM confirms the uniformity and narrow size distribution of the synthesized ZnO crystals.

Keywords zinc oxide, controlled-synthesis, nanoring

1 Introduction

ZnO, as an important functional oxide, is a direct wide band gap (3.37 eV) semi-conducting and piezoelectric material having many useful properties such as optical absorption and emission, conductivity, piezoelectricity, photo-catalysis, and sensitivity to gases. Different methods such as vapor-liquid-solid growth, thermal evaporation, thermal decomposition, electrochemical deposition and solution-phase processes have been introduced to prepare nano- or micro-scale ZnO particles with various morphologies [1–18]. Of these methods, the easy solution-based procedures may be the most simple and effective way to prepare well crystallized materials with uniform particle size distribution at a relatively low temperature. Moreover, the advantages of solution-based methods have also involved the remarkable influence of surfactants on the size and morphology of the final products. In this paper, a low-temperature, environmentally benign solution-phase approach to fabricate ZnO nanorings in the presence of commonly available polymer PAM-CTAC as crystal growth modifier was developed. The influence of experimental conditions such as concentration of PAM-CTAC and reactants, reaction temperature on the structure and morphology of as-products were investigated. A possible growth mechanism of ZnO nanorings in a mild aqueous solution was discussed.

Translated from *Chemical Journal of Chinese Universities*, 2008, 29(1): 28–32

Yin PENG (✉), Ling BAO
Anhui Key Laboratory of Functional Molecular Solids, College of Chemistry and Materials Science, Anhui Normal University, Wuhu 241000, China
E-mail: kimipeng@mail.ahnu.edu.cn

2 Experiments

2.1 Preparation

All chemicals including hexamethylenetetramine ($C_6H_{12}N_4$, HMT), $Zn(NO_3)_2 \cdot 2H_2O$ and poly (acrylamide-*co*-diallyldimethy- lammonium chloride) (PAM-CTAC) were of analytical grade and were used without further purification. In a typical procedure, 29.7 g $Zn(NO_3)_2 \cdot 2H_2O$, 14.0 g HMT and 1.0 g PAM-CTAC were dissolved in enough distilled water, to form 100 mL-solutions. Ten mL $Zn(NO_3)_2 \cdot 2H_2O$, 10 mL HMT and 30 mL PAM-CTAC aqueous solution were mixed in a 50-mL beaker under constant stirring. The mixture, which became milky right away, was stirred for 10 min and then transferred into a 250-mL flask. The solution was heated to 70°C with refluxing for 5 h without stirring and then air-cooled to room temperature. The resulting white product was thoroughly washed

with distilled water and dried at 60°C in a vacuum oven for further characterization.

2.2 Characterization

XRD patterns were recorded on a Rigaku D/Max 2200VPC X-Ray diffractometer with CuKα radiation ($\lambda = 1.540456$ nm) operating at 15 kV, 30 mA, scan speed of 0.02°/s and scan range of 20°–80°. SEM images were obtained on a Hitachi S-4800 microscope operating at 15 kV. TEM images were obtained on a JEOL JEM-2010 microscope operated at 200 kV. The selected area electron diffraction (SAED) patterns were obtained on a JEOL JEM-2010 microscope with an accelerating voltage of 200 kV. The photoluminescence (PL) spectra were recorded with an F-4500 spectrophotometer equipped with a 150-W xenon lamp as the excitation source at room temperature.

3 Results and discussion

3.1 Structure and morphology of ZnO products obtained

The phase purity of the products obtained in the presence of polyacrylamide (PAM) was examined by XRD measurement. All the peaks of the XRD pattern in Fig. 1 can be readily indexed to a pure hexagonal phase (JCPDS 36–1451) of ZnO nanorings. The morphology and structure of the products were examined with SEM. As shown in Fig. 1, the ZnO products obtained in the presence of PAM-CTAB consist almost entirely of uniform hexagonal ring-like and short rod-like structures. These nanorings have outer diameters of 360 nm, inner diameters of 220 nm and wall thicknesses of 70 nm. The selected area electron diffraction (SAED) pattern (the inset in Fig. 1) taken from a single nanoring can be indexed as a hexagonal wurtzite ZnO single crystal.

3.2 Influencing factors

3.2.1 Effect of PAM-CTAC concentration

When a smaller quantity of PAM-CTAC (0.06 $g \cdot L^{-1}$) is added, compact ZnO rods are obtained (Fig. 2). These rods assemble into one of two types of chrysanthemum structures (Fig. 2(a)). One type shows growth defects on top and the other exhibits a smooth top. Increasing the PAM-CTAC concentration from 0.06 $g \cdot L^{-1}$ to 0.3 $g \cdot L^{-1}$ affects the size and morphology of ZnO products as shown in Fig. 2(b). When the PAM-CTAC concentration is 0.6 $g \cdot L^{-1}$, a great change is observed in the shape of ZnO products obtained. The chrysanthemum structure

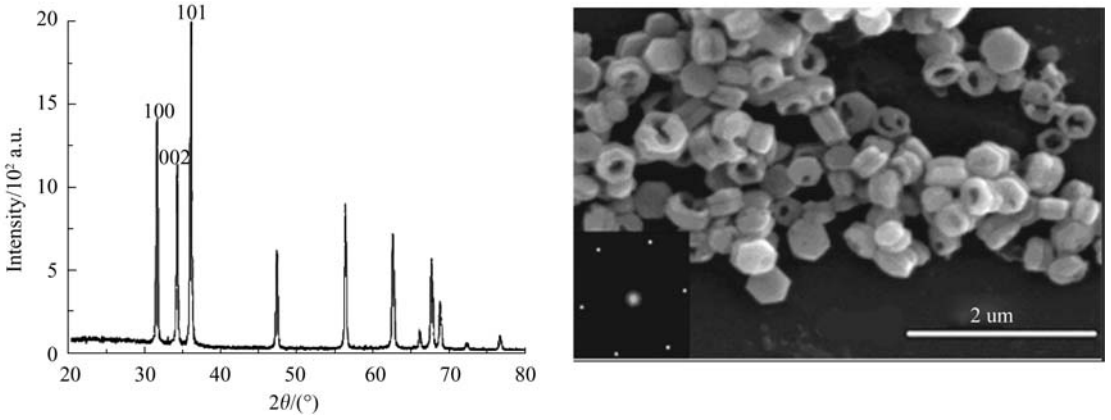

Fig. 1 XRD image and SEM image of ZnO product obtained at 70°C for 5 h (PAM-CTAC: 3.0 $g \cdot L^{-1}$, reactants: 1.0 $mol \cdot L^{-1}$), the in-set Figure is the SAED image of single ZnO nanoring

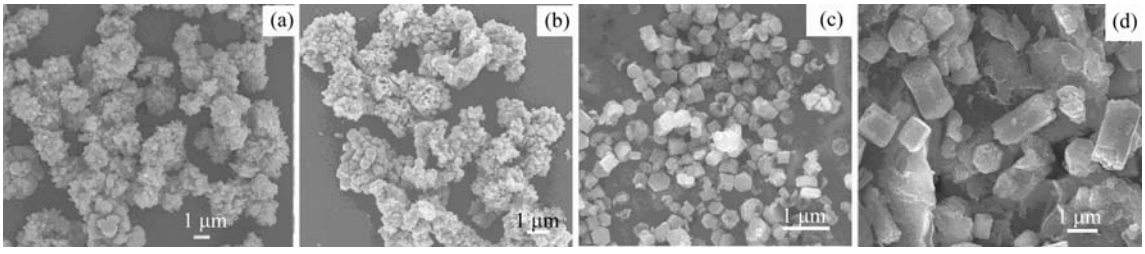

Fig. 2 SEM images of ZnO products obtained at 70°C for 5 h (reactants: 1.0 $mol \cdot L^{-1}$) in the different concentrations of PAM-CTAC: (a) 0.06; (b) 0.3; (c) 0.6 and (d) 9.0 $g \cdot L^{-1}$

completely disappears and some six-sided short-rods are obtained. At the same time, small nanorings appear as shown in Fig. 2(c). With further increase in the PAM-CTAC concentration, the number of the ring-like structure gradually increases and reaches a maximum at a PAM-CTAC concentration of 3.0 $g \cdot L^{-1}$ as shown in Fig. 1. It then decreases with continuous increase in the PAM-CTAC concentration. When the PAM-CTAC concentration reaches 9.0 $g \cdot L^{-1}$, the ZnO products obtained are small rod-like structures as shown in Fig. 2(d). The above results provide a simple approach to control the shape and size of ZnO products obtained by adjusting the PAM-CTAC concentration.

3.2.2 Effect of reactants concentration

When the reactant concentration is 0.2 $mol \cdot L^{-1}$, ZnO with hexagonal rod-like structures are obtained. At the same time, the small ZnO nanorings appear as shown in Fig. 3(a). When the reactant concentration is 0.6 $mol \cdot L^{-1}$, the number of nanorings increases but the main shape of ZnO obtained is hexagonal and rod-like as shown in Fig. 3(b). With further increase in the reactant concentration, the number of nanorings gradually increases and reaches a maximum at a reactant concentration of 1.0 $mol \cdot L^{-1}$ as shown in Fig. 1. Above 1.0 $mol \cdot L^{-1}$ reactant concentration, the number of nanorings deceases with increasing reactant concentration. When the reactant concentration reaches 2.0 $mol \cdot L^{-1}$, hexagonal rods are obtained with a few nanorings as shown in Fig. 3(c). At 4.0 $mol \cdot L^{-1}$ reactant concentration, all the ZnO obtained have rod-like structure and the size increases significantly as shown in Fig. 3(d). These results indicate that the size and morphology of ZnO products obtained can be effectively controlled by adjusting the concentration of the reactants.

3.2.3 Effect of reaction temperature

Between 40°C and 50°C, large and amorphous ZnO blocks are obtained. When the reaction temperature is 60°C, a small amount of the hexagonal short rods and nanorings appear as shown in Fig. 4(a). This result shows that PAM-CTAC begins to control the morphology of ZnO products obtained at 60°C. The number of nanorings increases significantly with increasing reaction temperature and reaches maximum at 70°C. Above 70°C, the number of nanorings starts to decline with further increase in reaction temperature. At 90°C, the ZnO products obtained are all hexagonal short rods with uniform size as shown in Fig. 4(b). No nanorings are obtained. Thus, the yield of nanorings initially increases with increasing temperature then decreases above a certain temperature. This result shows that the reaction temperature has a certain impact on the yield of nanorings.

The concentration of PAM-CTAC and reactants and the reaction temperature have a certain impact on the structure and morphology of ZnO products obtained but PAM-CTAC plays a key role on the formation of ZnO nanorings. Without PAM-CTAC, no nanorings are obtained despite altered experimental conditions. The size and morphology of ZnO products obtained can be effectively controlled by changing the PAM-CTAC

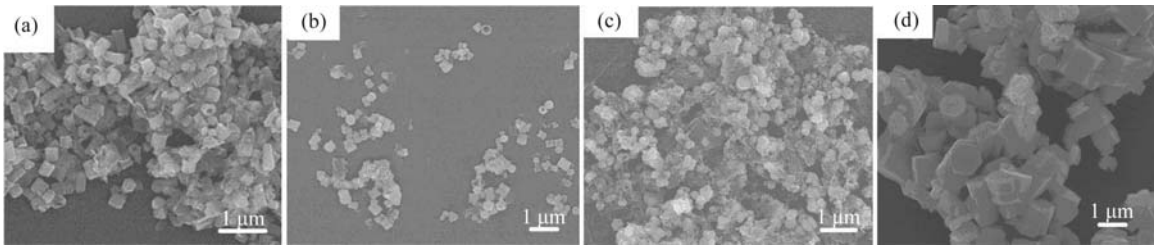

Fig. 3 SEM images of ZnO products obtained at 70°C for 5 h (PAM-CTAC: 3.0 $g \cdot L^{-1}$) with reactants concentration: (a) 0.2; (b) 0.6; (c) 2.0 and (d) 4.0 $mol \cdot L^{-1}$

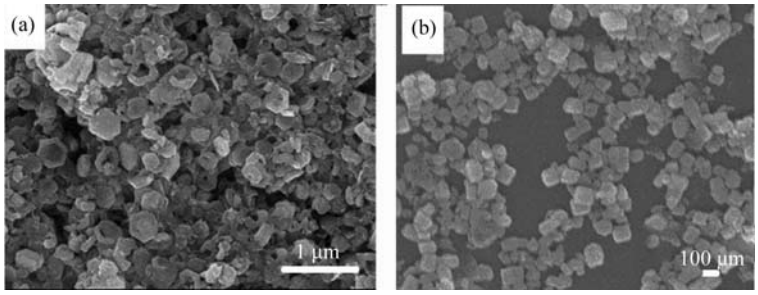

Fig. 4 SEM images of ZnO products obtained at (a) 60°C and (b) 90°C for 5 h (reactants: 1.0 $mol \cdot L^{-1}$, PAM-CTAC: 3.0 $g \cdot L^{-1}$)

concentration. In order to synthesize high-yield ZnO nanorings, the optimal reaction conditions are as follows: reaction temperature is 70°C, the concentration of reactants and PAM-CTAC are 1.0 mol·L^{-1} and 3.0 g·L^{-1}, respectively.

3.3 The formation mechanism of ZnO nanorings

To investigate the formation mechanism of ZnO nanorings, reaction time-dependent experiments are carried out at 70°C. As shown in Fig. 5(a), ZnO products obtained are discus-like structure when the reaction time is 0.5 h. As shown in Fig. 5(b), ZnO products obtained after 1 h are mainly hexagonal short rods but no nanorings appear. After 1.5 h, some nanorings appear as shown in Fig. 5(c). However, some discus-like structures are still obtained. This result implies that ring-like and rod-like structures may come from discus-like structures. When the reaction time reaches 2 h, discus-like structures completely disappear and the ZnO products obtained are all nanorings and hexagonal short rods as shown in Fig. 5(d). After 2 h, the morphology and size of ZnO products obtained are unchanged until a reaction time of 8 h is achieved as shown in Figs. 5(e) and 5(f).

Zinc nitrate and HMT undergo the following reactions in solution:

$$(CH_2)_6N_4 + 6H_2O \rightarrow 6HCHO + 4NH_3 \quad (1)$$

$$NH_3 + H_2O \rightarrow NH_4^+ + OH^- \quad (2)$$

$$2OH^- + Zn^{2+} \rightarrow ZnO(s) + H_2O \quad (3)$$

At the initial reaction stage, the complexes $[Zn(H_2O)_2(HMTA)_2](NO_3)_2$ and $[Zn(H_2O)_4(HMTA)_2](NO_3)_2$ may exist [19–21].

$$Zn(NO_3)_2 + 2H_2O + 2HMTA \rightarrow [Zn(H_2O)_2(HMTA)_2](NO_3)_2 \quad (4)$$

$$Zn(NO_3)_2 + 4H_2O + 2HMTA \rightarrow [Zn(H_2O)_4(HMTA)_2](NO_3)_2 \quad (5)$$

These organic metal complexes act as nuclei which grow and form discus-like precursors. With increasing reaction temperature and reaction time, unstable organic metal complexes start to dissociate into HMT and other products. The OH^- from the HMT hydrolysis reacts with Zn^{2+} in the solution and forms ZnO nuclei on the surface of the organic metal complex. With the organic metal complexes continuously decomposing, the ZnO nuclei grow gradually. Finally, the organic complexes completely dissociate and ZnO nanorings are formed.

The velocities for growth under solution conditions are reported to be $V_{001} > V_{010} > V_{100}$. Therefore, in the pure solution, ZnO grows most likely along the C-axis to become the long rod structure. PAM-CTAC contains in the side chain a large number of amide ligands that are able to coordinate with Zn^{2+} ions that is on the weakly exposed (001) face leading to a lowering of surface energy and inhibition of growth along this direction [22–24]. Therefore, during the complexes' constant decomposition and the ZnO crystal growth process, PAM-CTAC inhibits ZnO crystal growth along the C-axis direction and ultimately ZnO nanorings are formed.

3.4 Photoluminescence (PL) spectrum

A room-temperature PL spectrum of ZnO products obtained is shown in Fig. 6. The strong sharp peak around 390 nm is attributed to the excitation transitions,

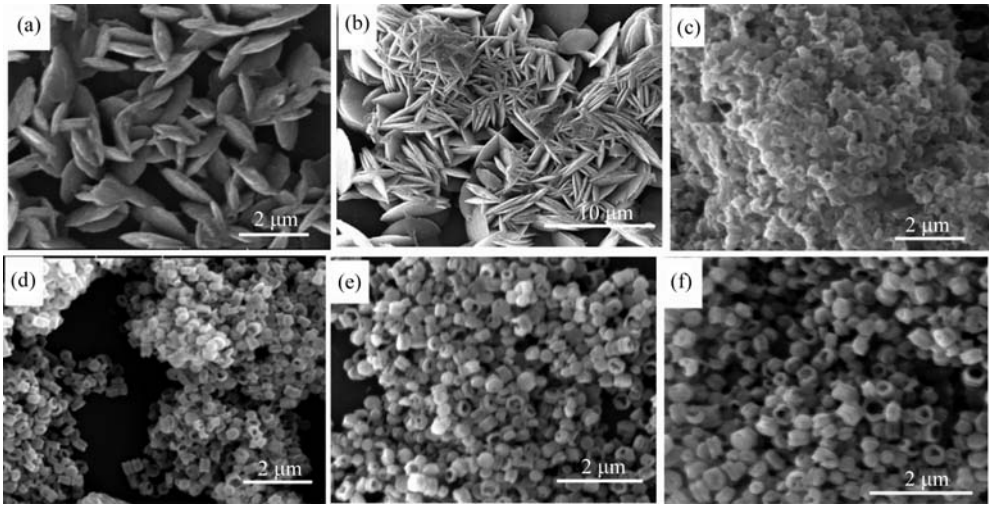

Fig. 5 SEM images of ZnO products obtained at 70°C for (a) 0.5; (b) 1; (c) 1.5; (d) 2; (e) 2.5 and (f) 8 h (PAM-CTAC: 3.0 g·L^{-1}, reactants: 1.0 mol·L^{-1})

which is a ZnO intrinsic emission peak. The weak emission peak centered at 470 nm corresponds to the deep level or trap-state emission which is related to structural defects or impurities. The full width at half-maximum (FWHM) of the UV emission of ZnO products obtained is calculated to be approximately 7 nm, which is much narrower than that of commercial ZnO bulk crystals (18 nm), indicating that the ZnO products obtained have a high optical property[25]. The narrow FWHM confirms the uniformity and narrow size distribution of the synthesized ZnO crystals.

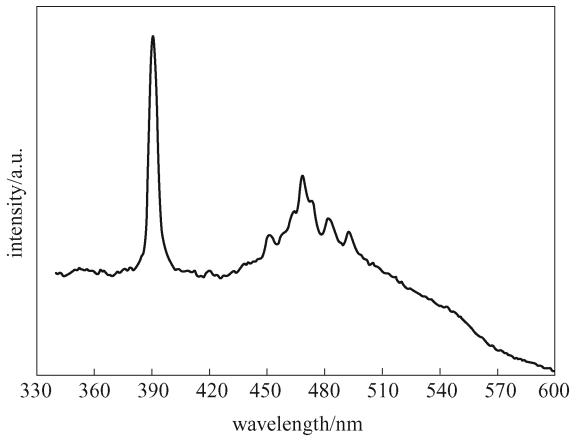

Fig. 6 A room temperature photoluminescence spectrum of the obtained ZnO nanorings

4 Conclusions

A mild aqueous solution route to prepare the different morphologies of ZnO crystals with high crystallinity and uniform size and shape was developed by polymer-controlled crystallization. Polymer-directed crystal growth can provide promising ways for rational synthesis of various ordered inorganic and inorganic-organic hybrid materials with complex form and structural specialty. The hexagonal nanoring crystal obtained is a new member in the family of ZnO nanostructures. The simplicity of the mild solution process, the low cost, the availability of raw materials and the nonrequirement of a catalyst are advantages favoring the scaling-up of the novel method. Further work is needed to better understand the detailed mechanism involving a synergistic effect of the mutual interactions between functionalities of the polymer and inorganic species. The novel ZnO nanostructure may be used as building blocks for photonic and electronic nano-device applications, e.g., in EUV applications or for "whispering gallery" mode micro-lasers.

Acknowledgements This work was supported by the National Natural Science Foundation of China (Grant No. 20671002) and the Anhui Province Outstanding Youth Fund (04046065). Author thanks the Anhui Key Laboratory of Functional Molecular Solids, College of Chemistry and Materials Science, Anhui Normal University for granting a research fellowship.

References

1. Pan Z W, Dai Z R, Wang Z L. Nanobelts of semiconducting oxides. Science, 2001, 291: 1947–1949
2. Kong X Y, Wang Z L. Spontaneous polarization-induced nanohelixes, nanosprings, and nanorings of piezoelectric nanobelts. Nano Let., 2003, 3(12): 1625–1361
3. Huang M H, Mao S, Feick H, Yan H Q, Wu Y Y, Kind H, Weber E, Russo R, Yang P D. Room-temperature ultraviolet nanowire nanolasers. Science, 2001, 292: 1897–1899
4. Meng X M, Lee C S, Lee S T, Hu J Q. Thermal reduction route to the fabrication of coaxial Zn/ZnO nanocables and ZnO nanotubes. Chem Mater, 2003, 15(1): 305–308
5. Xia Y, Yang P, Sun Y, Wu Y, Mayers B, Gates B, Yin Y, Kim F, Yan H. One-dimensional nanostructures: synthesis, characterization and applications. Adv Mater, 2003, 15(5): 353–389
6. Vayssieres L. Growth of arrayed nanorods and nanowires of ZnO from aqueous solutions. Adv Mater, 2003, 15(5): 464–466
7. Peterson R B, Fields C L, Gregg B A. Epitaxial chemical deposition of ZnO nanocolumns from NaOH solutions. Langmuir, 2004, 20(12): 5114–5118
8. Liu B, Zeng H C. Hydrothermal synthesis of ZnO nanorods in the diameter regime of 50 nm. J Am Chem Soc, 2003, 125(15): 4430–4431
9. Li F, Ding Y, Gao P X, Xin X Q, Wang Z L. Single-crystal hexagonal disks and rings of ZnO: low-temperature, Large-scale synthesis and growth mechanism. Angew Chem Int Ed, 2004, 43(39): 5238–5242
10. Zhong X H, Knoll W. Morphology-controlled large-scale synthesis of ZnO nanocrystals from bulk ZnO. Chem Commun, 2005, 9: 1158–1160
11. Govender K, Boyle D S, Kenway P B, O'Brien P. Understanding the factors that govern the deposition and morphology of thin films of ZnO from aqueous solution. J Mater Chem, 2004, 14(16): 2575–2591
12. Kong X Y, Ding Y, Yang R, Wang Z L. Single-crystal nanorings formed by epitaxial self-coiling of polar nanobelts. Science, 2004, 303: 1348–1351
13. Gao P M, Lao C S, Hughes W L, Wang Z L. Three-dimensional interconnected nanowire networks of ZnO. Chem Phys Let, 2005, 408(1–3): 174–178
14. Gao P X, Wang Z L. Nanopropeller arrays of zinc oxide. Appl Phys Let, 2004, 84(15): 2883–2885
15. Buha J, Djerdj I, Niederberger M. Nonaqueous synthesis of nanocrystalline indium oxide and zinc oxide in the oxygen-free solvent acetonitrile. Cryst Growth & Des, 2007, 7(1): 113–116
16. Ghoshal T, Kar S, Chaudhuri S. ZnO doughnuts: controlled synthesis, growth mechanism and optical properties. Cryst Growth & Des, 2007, 7(1): 136–141
17. Peng Y, Xu A W, Deng B, Antonietti M, CÖlfen H. Polymer-controlled crystallization of zinc oxide hexagonal nanorings and disks. J Phys Chem B, 2006, 110(7): 2988–2993
18. Zou Q, Zhang Z S, Li H Y, Hu M, Qin Y X, Liu Z G. Synthesis and characterization of ZnO nanobelts via the reaction between zinc acetate and polyvinyl alcohol. Chen J Chin Uni, 2006, 27(7): 1211–1217 (in Chinese)
19. Chou K S, Chen W H, Huang CS. Precipitation studies of hydrous zinc oxide colloids. J Chin Inst Chem Eng, 1990, 21(6): 327–334
20. Grodzicki Z, Szlky E. Hydrates of Zn(II) HMTA salts: part II. Polish J Chem, 1984, 58: 999–1004
21. Grodzicki Z, Szlky E. Hydrates of Zn(II) HMTA salts: part III. Polish J Chem, 1984, 58: 1009–1013
22. Taubert A, Palms D, Weiss Ö, Piccini M T, Batchelder D N. Polymer-assisted control of particle morphology and particle

size of zinc oxide precipitated from aqueous solution. Chem Mater, 2002, 14: 2594–2601
23. Taubert A, Kübel C, Martin D C. Polymer-induced microstructure variation in zinc oxide crystals precipitated from aqueous solution. J Phys Chem B, 2003, 107(12): 2660–2666
24. Tian Z R, Voigt J A, Liu J, Mckenzie B, Mcdermott M J, Rodriguez M A, Konishi H, Xu H F. Complex and oriented ZnO nanostructures. Nat Mater, 2003, 2(12): 821–826
25. Geng C, Jiang Y, Yao Y, Meng X, Zapien J A, Lee C S, Lifshitz Y, Lee S T. Well-aligned ZnO nanowire arrays fabricated on silicon substrates.Adv Funct Mater, 2004, 14(6): 589–594